# Photoswitchable Radical State in Nanoporous Metal–Organic Framework Films with Embedded Hexaarylbiimidazole

Yidong Liu, Yunzhe Jiang, and Lars Heinke*

**ABSTRACT:** Photoresponsive materials enable dynamic remote control of their fundamental properties. The incorporation of photochromic molecules in nanoporous metal–organic frameworks (MOFs) provides a unique opportunity to tailor the material properties, including the interaction between the MOF host and guest molecules in the pores. Here, a MOF film of type HKUST-1 with embedded hexaarylbiimidazole (HABI), undergoing reversible light-induced reactions between the stable dimer state and the metastable radical state, is presented. The switching between the dimer and radical form is shown by infrared, UV–vis, and electron paramagnetic resonance (EPR) spectroscopy. By transient uptake experiments with ethanol and methanol as probe molecules, we show that the dimer-radical switching impacts the host–guest interaction and, in particular, modifies the uptake amount and diffusion coefficient of the guest molecules. For ethanol, the diffusion slows down by 75%. This research presents the first MOF material with photoswitchable (meta)stable dimer and radical molecules, and it contributes to the advancement of photoresponsive nanoporous materials.

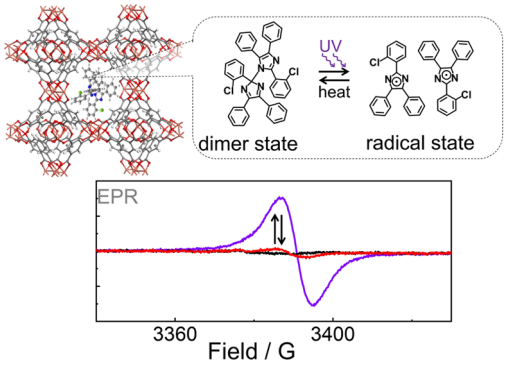


## INTRODUCTION

Smart and adaptive materials are required for advanced applications.[1,2] A large research focus is on smart materials whose structural and physical properties can be controlled remotely.[3,4] Due to their ability to change their shape and properties upon excitation by light, photochromic molecules play a crucial role in conferring stimuli-responsive properties to materials. Commonly used photochromic molecules include spiropyran (SP), azobenzene (AB), and diarylethylene (DAE).[5,6] In contrast to these common photochromic molecules, hexaarylbiimidazole[7] (HABI) and its derivatives can reversibly transfer from a dimer state to a radical state (Figure 1). Through UV light irradiation, one HABI molecule can undergo a photochromic reaction and split into two triphenylimidazole radicals (TPIRs). At elevated temperature, the two radicals can again (re)combine to a dimer. This photochromic property allows HABI to be used as photoinitiators and in self-healing materials.[8,9] Furthermore, through the integration of HABI, materials can be endowed with corresponding stimuli-responsive properties and applied as photoresponsive actuators[10] and nonvolatile memory.[11]

Metal–organic frameworks (MOFs) are attractive hosts for photochromic molecules. MOFs are made of metal nodes linked by organic linker molecules.[12] MOFs possess a nanoporous and crystalline structure as well as high structural variability. Through covalent linkage or loading in the pores, responsive molecules can be incorporated in the MOF, resulting in stimuli-responsive materials.[13,14] This allows MOFs to react to external stimuli such as pressure,[15] heat,[16] humidity[17] or light irradiation,[18,19] making them suitable for advanced and smart applications. In particular, the incorporation of photochromic molecules into MOFs provides a promising strategy to realize MOFs with remote-controllable properties,[20−22] enabling researchers to develop various applications such as drug delivery,[23] sensing,[24] and catalysis[25] as well as gas adsorption and diffusion.[26]

In contrast to conventional hydrothermal or solvothermal techniques used to prepare MOFs in the form of powders,[27] surface-mounted metal–organic frameworks (SURMOFs) are synthesized in a layer-by-layer (LBL) manner directly on the substrate surface, resulting in the formation of thin and homogeneous MOF films.[28] The transparency of SURMOFs[29] allows for the characterization of their optical properties using UV–vis spectroscopy in transmission mode. Additionally, the precise quantification of the uptake of guest molecules from the gas phase can be achieved using a quartz crystal microbalance (QCM).[30,31]

Here, we present a nanoporous SURMOF film functionalized with photochromic *o*-Cl-HABI molecules. The SURMOF host structure is of type HKUST-1, which was chosen

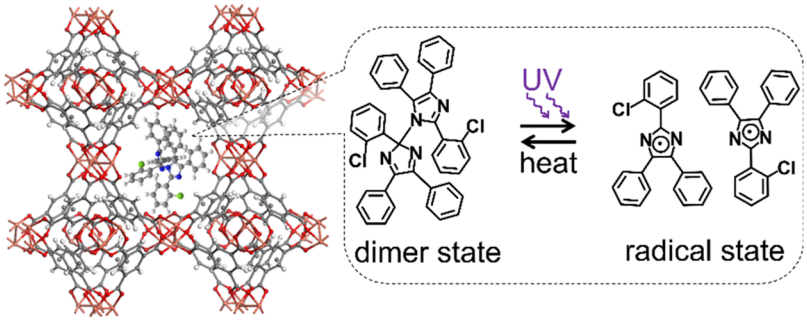


**Figure 1.** Sketch of HKUST-1 with the embedded photochromic *o*-Cl-HABI in the pore. Under UV-light irradiation, *o*-Cl-HABI dissociates into a pair of TPIRs. Such a radical pair can recombine to *o*-Cl-HABI, accelerated at an elevated temperature.

due to its good stability, high surface area, and appropriate pore size.[32] In addition, well-defined HKUST-1 films can be grown with a low defect density.[29,33] The *o*-Cl-HABI molecule in the pores can undergo light-induced reversible transition between the dimer and the radical state (Figure 1), shown by infrared, UV−vis, and electron paramagnetic resonance (EPR) spectroscopy. Uptake experiments with ethanol and methanol as the guest molecules show the remote-controlled switching of the uptake amount and rates as response to the *o*-Cl-HABI switching

## EXPERIMENTAL SECTION

**Materials.** The chemicals, i.e., trimesic acid (98%, Alfa Aesar), copper(II) acetate (99.9%, Alfa Aesar), 11-mercapto-1-undecanol (99%, Sigma-Aldrich), *o*-Cl-HABI (98%, TCI), methanol (99.5%, VWR Chemicals), and ethanol (99.5%, VWR Chemicals), were purchased from Alfa Aesar and VWR and were used without further purification. The substrates for the MOF films are gold-coated QCM sensors with a resonance frequency of 5 MHz from Q-Sense, purchased from Biolin Scientific, quartz glass sheets from GVB Solutions in Glass, and gold-coated silicon wafer purchased from Georg Albert PVD coatings.

**MOF Film Synthesis and Photoswitch Embedment.** HKUST-1 SURMOFs were prepared in a layer-by-layer fashion by alternatively dipping the substrates in the solutions of the MOF components, i.e., ethanolic 1 mM copper(II) acetate solution and ethanolic 0.2 mM trimesic acid (also known as benzene-1,3,5-tricarboxylic acid) solution, using a dipping robot as reported.[29] The dipping times were 10 min for the copper acetate solution and 15 min for the trimesic acid solution, each followed by a dipping step in pure ethanol for 2 min to remove residual reactants. The samples were prepared in 80 synthesis cycles. The SURMOF substrates are quartz glass sheets (2 cm × 2 cm) functionalized by oxygen plasma treatment (for UV−vis experiments), gold-coated silicon wafer substrates (2 cm × 2 cm, for IRRAS experiments), or gold-coated QCM sensors (for uptake experiments), functionalized with an 11-mercapto-1-undecanol self-assembled monolayer. Pure *o*-Cl-HABI films were prepared by a spin-coating process where the quartz substrate (for UV−vis experiments) and gold-coated silicon substrate (for IRRAS experiments) substrates were first rinsed with ethanol and later dried with $N_2$ flow; then the pretreated substrates were placed on a vacuum chuck and subsequently spin coated in a continuous mode during the addition of 50 $\mu$L of 10 mM *o*-Cl-HABI ethanolic solution for 10 s at 500 rpm spin-coating speed. The spin-coating process was repeated 3−5 times. The ethanol evaporates, leaving a pure HABI film.

The embedment of the *o*-Cl-HABI photochromic molecules in the pores of the HKUST-1 SURMOF film was performed by soaking the MOF sample in 5 mM *o*-Cl-HABI ethanolic solution at room temperature for 24 h. Afterward, the sample surface was briefly rinsed with ethanol, and the sample was dried in a flow of pure nitrogen.

**Characterizations.** The X-ray diffraction (XRD) data of the MOF films were recorded with a Bruker D8 ADVANCE X-ray diffractometer with Cu K$\alpha$ radiation ($\lambda$ = 0.154 nm) and an out-of-plane (Bragg−Brentano) geometry. The scanning electron microscopy (SEM combined with energy-dispersive X-ray (EDX) spectroscopy) measurements were performed on a TESCAN VEGA3. To avoid charging effects, all samples were coated with a 3−4 nm thick platinum film before recording the SEM images. UV−vis spectroscopy in transmission mode was explored with a Cary5000 spectrometer with an UMA unit from Agilent. Infrared reflection−absorption (IRRA) spectroscopy was performed with a Bruker Vertex 80 spectrometer with a resolution of 2 $cm^{-1}$. The transient uptake amount of the guest molecules (here, methanol and ethanol) was quantified by using a Q-Sense E4 QCM-D, working at a resonance frequency of approximately 5 MHz. The QCM cell was connected to the gas flow system with nitrogen as carrier gas.[31] Before each uptake experiment, the sample was activated in pure nitrogen flow at 65 °C until a stable baseline was reached (typically after a few hours), and the MOF pores were empty. The electron paramagnetic resonance (EPR) data were recorded with a Bruker EMXnano EPR system (see refs 34 and 35).

## RESULTS AND DISCUSSION

The MOF thin films are prepared in a layer-by-layer fashion on the solid substrate. The SURMOF film was loaded with *o*-Cl-HABI by immersing the SURMOF sample in an ethanolic *o*-Cl-HABI solution overnight. Following loading, the ethanol solvent evaporated, leaving HABI in the pores. For the photoisomerization of *o*-Cl-HABI, the samples were irradiated with UV light and thermally relaxed, accelerated by heat treatment (at approximately 100 °C in air for 10 min).

The structure of the HKUST-1 SURMOF film was investigated before and after loading with *o*-Cl-HABI, using X-ray diffraction (XRD) in an out-of-plane geometry. The diffractograms of the SURMOF film are shown in Figure 2. The XRD pattern shows only peaks of the (100) orientation of

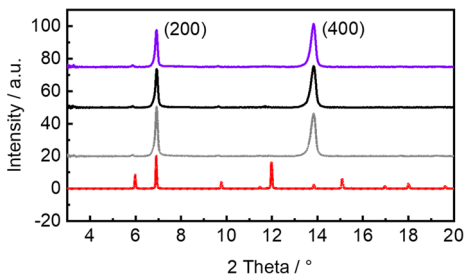


**Figure 2.** X-ray diffractograms of the pristine HKUST-1 SURMOF (gray) and after *o*-Cl-HABI-loading, before (black) and after (violet) UV irradiation. The diffractogram calculated for HKUST-1 powder is shown in red. The experimentally observed diffraction peaks are labeled.

HKUST-1, as observed for HKUST-1 SURMOF on different substrates before.[29,36−38] There, all peaks perpendicular to the [001] direction of HKUST-1 can be seen in the XRD with in-plane geometry.[36,38] Thus, the data indicate that the film has a crystalline HKUST-1 structure, which is primarily oriented in the [100] direction perpendicular to the substrate surface.

Upon loading the HKUST-1 SURMOF with *o*-Cl-HABI, a change in the intensity ratio of the XRD reflections was observed. In particular, the ratio of the intensities for the (200) peak compared to the (400) peak decreased from 1.16 to 0.93, showing a change in the XRD form factor and indicating successful loading of the guest molecules (*o*-Cl-HABI). Furthermore, the XRD patterns were used to compare the *o*-Cl-HABI@HKUST-1 film before and after UV light irradiation. The ratio of the peak intensities, (200) versus (400), was barely affected by the UV-light irradiation, i.e., it is 0.93 and 0.90 before and after UV light. It suggests that the MOF structure was not affected by the photoinduced reaction of the guest molecule (see below).

Scanning electron microscopy (SEM) was employed to investigate the film morphology (Figure S1). The images of the pristine HKUST-1 MOF film and the *o*-Cl-HABI@HKUST-1 film indicate that the film covers the substrate surface homogeneously. The film is composed of crystallites with a size of ≈0.2 $\mu$m and has a thickness of ≈0.2 $\mu$m.

The EDX analysis (Figure S6) shows that, on average, 4.3 HABI molecules are loaded in each HKUST-1 unit cell, corresponding to approximately 1 HABI molecules embedded in each large pore of HKUST-1.

The photoinduced reaction of *o*-Cl-HABI@HKUST-1 was explored using UV−vis spectroscopy (Figure 3). The spectra of the pure *o*-Cl-HABI film (Figure S2) are used as reference. Initially, *o*-Cl-HABI exists in the thermodynamically stable dimer state and absorbs light predominantly in the UV range. Upon UV irradiation with a wavelength of 365 nm, the UV−vis spectra exhibit small absorption bands at 303 and 443 nm. For a better visibility, the differential spectra with the pristine spectra as reference are shown as insets in Figures 3b and S2. This spectral change indicates that *o*-Cl-HABI embedded in the MOF pores undergoes transformation from the dimer state to the radical state upon UV-irradiation, similar to the pure material.[11] These light-induced changes of the spectrum of the *o*-Cl-HABI@HKUST-1 film was observed in all prepared samples. To explore the stability of *o*-Cl-HABI within the HKUST-1 pores, we conducted transient UV−vis spectroscopic analyses before and after UV irradiation with the HABI molecules in solution, as pure film (no MOF) and embedded in the MOF pores. Figure S3 shows the transient behavior where the monoexponential time constants $\tau$ describing the radical-to-dimer kinetics were determined. The time constants are approximately 230 s, 27.7 h, and 27.4 h for the TPIRs' dimerization in the ethanolic solution, in the pure film (no MOF), and in the pores of HKUST-1, respectively.

Infrared reflection absorption spectroscopy (IRRAS) was used to quantitatively analyze the photoinduced reaction of *o*-Cl-HABI@HKUST-1. Figure 3b displays the IRRA spectra of this film before and after UV irradiation. The strongest bands at 1653 and 1385 cm$^{-1}$ can be assigned to the asymmetric stretching mode of $COO^-$ and symmetric stretching mode of C−O, as part of HKUST-1.[39] A comparison between pristine HKUST-1 and *o*-Cl-HABI@HKUST-1 reveals a new band at 915 cm$^{-1}$, which is not overlapped by other vibrations, indicating the successful loading of the guest photochromic

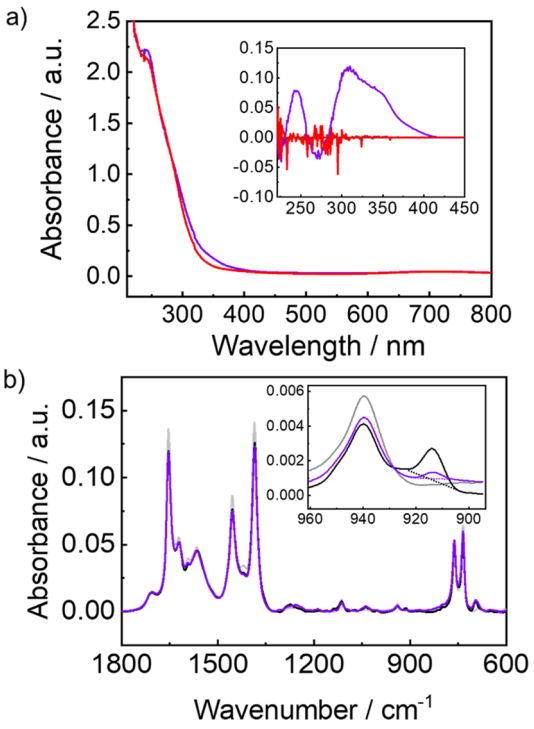


**Figure 3.** (a) UV−vis spectra of the pristine *o*-Cl-HABI@HKUST-1 film (black), after UV irradiation for 10 min (violet), and after heat treatment for 10 min (red). The inset shows the differential spectra with the pristine spectrum as reference. (b) IRRAS of the unloaded HKUST-1 film (gray) and HKUST-1 film loaded with *o*-Cl-HABI (black) and subsequently irradiated with UV light for 10 min (violet).

molecules. This can be used to quantify the HABI photoswitching yield. Initially, *o*-Cl-HABI@HKUST-1 is in the 100% dimer state. After UV irradiation, the intensity of the band at 915 cm$^{-1}$ decreased to 16.4% of its initial area. This indicates that ≈84% *o*-Cl-HABI transforms from the dimer state to the radical state. This switching yield is in line with ref 40. In Figure S4, the IRRA spectra of pure *o*-Cl-HABI before and after UV irradiation are presented as reference. A similar change of the band at 915 cm$^{-1}$ is found there, indicating that *o*-Cl-HABI in the pores of the HKUST-1 SURMOF film undergoes a photochromic reaction upon UV irradiation, like the pure photoswitch.

The photoinduced dissociation of *o*-Cl-HABI, leading to the formation of radicals in TPIRs, was explored by electron paramagnetic resonance (EPR). The *o*-Cl-HABI@HKUST-1 film exhibited no EPR signal in the pristine state (Figure 4). This shows that the pristine *o*-Cl-HABI@HKUST-1 possesses no unpaired electrons. In contrast, a strong EPR signal was observed after UV light irradiation. The determined *g*-value was 2.0036. This indicates *o*-Cl-HABI in HKUST-1 undergoes a photoinduced reaction, causing unpaired electrons. The EPR signal disappears again after heat treatment. Based on these EPR findings, it can be concluded that the reversible conversion between *o*-Cl-HABI and the TPIRs can be achieved through alternating UV light irradiation and heating to a temperature of ≈100 °C. This means that the HABI molecule in the MOF pores can be reversibly switched between the dimer state and the radical state.

For exploring the effect of HABI photoswitching on the interaction with guest molecules, adsorption and diffusion experiments with ethanol and methanol as probe molecules

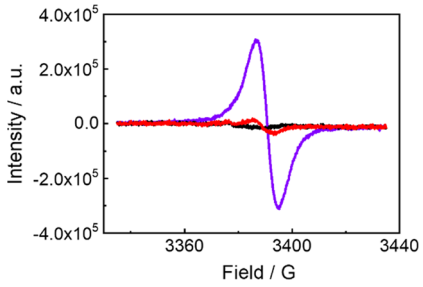


**Figure 4.** EPR spectrum of the pristine *o*-Cl-HABI@HKUST-1 film (black), after UV irradiation for 10 min (violet), and after heat treatment (100 °C for 10 min, red). The *g*-value was determined by the center of the two peaks of the EPR spectrum at 3390.8 G.

were performed. The transient uptake was recorded with a QCM. During the uptake experiments, the HABI@MOF film was irradiated with UV light and thermally relaxed. The transient uptake data of ethanol (Figure 5a) shows that the

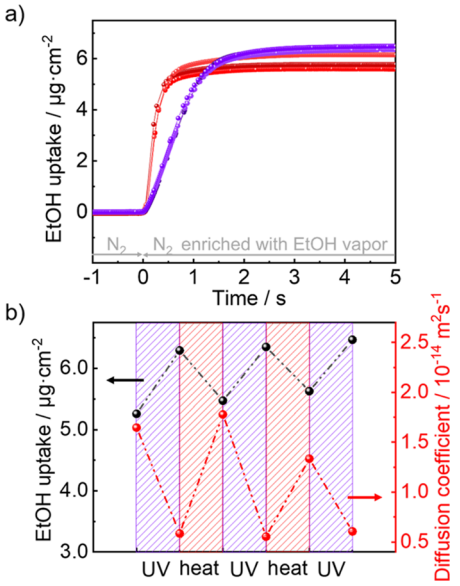


**Figure 5.** (a) Transient ethanol (EtOH) uptake for three switching cycles by the *o*-Cl-HABI@HKUST-1 film measured by QCM. The sample is in the dimer state (i.e., without irradiation, red) and in the radical state (after UV irradiation, violet). (b) Ethanol uptake amount (black) and diffusion coefficients (red) for three switching cycles. Violet indicates the UV-light irradiation, and red indicates the heat treatment.

ethanol uptake amount by the UV-irradiated *o*-Cl-HABI@HKUST-1 film (i.e., in the radical state) is higher than by the pristine sample. In addition, the uptake rate in the radical state is slower than that in the pristine state. Each uptake experiment was performed 3 times. The average uptake amount by the sample in the dimer form was 5.5 ± 0.2 $\mu$g cm$^{-2}$ and 6.4 ± 0.1 $\mu$g cm$^{-2}$ for the sample in the radical state. (The errors are the standard deviations of the three experiments.) This means that the dimer-to-radical-photoswitching increases the adsorption amount by ≈16%. The uptake data using methanol as probe molecule are shown in Figure S5b. The dimer-to-radical photoswitching increases the methanol adsorption amount by ≈12%.

An in-depth examination of the rates of the mass transfer (Figure 5b) was conducted by describing the experimental data with the solution of Fick's second law for a thin homogeneous film (here with a thickness of 0.2 $\mu$m) and an instant change of the surface concentration.[26,41,42] The obtained diffusion coefficient for ethanol in the MOF with HABI in the dimer state is (6.6 ± 0.9) × 10$^{-14}$ m$^2$ s$^{-1}$, whereas the diffusion coefficient for ethanol in the MOF with HABI in the radical state is (1.7 ± 0.2) × 10$^{-14}$ m$^2$ s$^{-1}$. This means that the diffusion coefficient drops significantly by 75%. The decrease in the diffusion coefficient is in line with the increased uptake amount. We believe that both the increase of the uptake amount and the decrease of the diffusion rate are caused by the stronger polar (attractive) interaction of the probe molecules with TPIR compared to HABI in the pores. Such polar (dipole−dipole) interaction has been observed for such probe molecules and other photoswitchable MOFs.[43,44]

It should be noted that the uptake processes are rather fast, indicating the absence of defects and surface barriers for the mass transfer.[45−48] The data also indicate that no surface barriers (which are explored for HKUST-1 SURMOF before[33,49]) are formed during the HABI loading, UV irradiation or heat treatment in air.

## CONCLUSIONS

In summary, we present a new photoswitchable nanoporous material by embedding *o*-Cl-HABI in a SURMOF film of the type HKUST-1. *o*-Cl-HABI can undergo a photoinduced reaction in the pores, so that the material can be switched between a thermodynamically stable dimer state and a metastable radical state. The creation and extinction of the radicals were verified by EPR. We show that the switching between both states modifies the adsorption and diffusion properties in the pores. We believe that this strategy for constructing stimuli-responsive MOFs with a photoswitchable radical state may have great potential in the field of catalysis and future smart materials like remote-control sensors.

## AUTHOR INFORMATION


### Corresponding Author

**Lars Heinke** − *Institute of Functional Interfaces (IFG), Karlsruhe Institute of Technology (KIT), 76344 Eggenstein-Leopoldshafen, Germany*; orcid.org/0000-0002-1439-9695; Email: Lars.Heinke@KIT.edu

### Authors

**Yidong Liu** − *Institute of Functional Interfaces (IFG), Karlsruhe Institute of Technology (KIT), 76344 Eggenstein-Leopoldshafen, Germany*

**Yunzhe Jiang** − *Institute of Functional Interfaces (IFG), Karlsruhe Institute of Technology (KIT), 76344 Eggenstein-Leopoldshafen, Germany*


### Notes

The authors declare no competing financial interest.

## ACKNOWLEDGMENTS

We thank the Deutsche Forschungsgemeinschaft (DFG, HE 7036/5) and the China Scholarship Council (CSC) for financial support. We gratefully thank Manuel Tsotsalas and Yi (Roy) Luo for their generous support with the EPR experiments and Abhinav Chandresh for the help with the EDX measurements.

## REFERENCES

(1) Soto, F.; Karshalev, E.; Zhang, F. Y.; de Avila, B. E. F.; Nourhani, A.; Wang, J. Smart Materials for Microrobots. *Chem. Rev.* **2022**, *122* (5), 5365−5403.

(2) Maity, C.; Das, N. Alginate-based smart materials and their application: recent advances and perspectives. *Top. Curr. Chem.* **2022**, *380*, 1−67.

(3) Singha, K.; Kumar, J.; Pandit, P. Recent advancements in wearable & smart textiles: An overview. *Mater. Today: Proc.* **2019**, *16*, 1518−1523.

(4) Chan, A.; Orme, R. P.; Fricker, R. A.; Roach, P. Remote and local control of stimuli responsive materials for therapeutic applications. *Adv. drug delivery rev.* **2013**, *65* (4), 497−514.

(5) Tsujioka, T.; Irie, M. Electrical functions of photochromic molecules. *J. Photochem. Photobiol., C* **2010**, *11* (1), 1−14.

(6) Bandara, H. M.; Burdette, S. C. Photoisomerization in different classes of azobenzene. *Chem. Soc. Rev.* **2012**, *41* (5), 1809−25.

(7) Dessauer, R. *Photochemistry, History and Commercial Applications of Hexaarylbiimidazoles: All about HABIs*; Elsevier: 2006.

(8) Ahn, D.; Zavada, S. R.; Scott, T. F. Rapid, photomediated healing of hexaarylbiimidazole-based covalently cross-linked gels. *Chem. Mater.* **2017**, *29* (16), 7023−7031.

(9) Ahn, D.; Sathe, S. S.; Clarkson, B. H.; Scott, T. F. Hexaarylbiimidazoles as visible light thiol-ene photoinitiators. *Dent. Mater.* **2015**, *31* (9), 1075−1089.

(10) Jia, S.; Graham, B.; Capuano, B.; Tan, A.; Hawley, A.; Boyd, B. J. Hexaarylbiimidazoles (HABI)-functionalized lyotropic liquid crystalline systems as visible light-responsive materials. *J. Colloid Interface Sci.* **2020**, *579*, 379−390.

(11) Liu, Y.; Yang, Y.; Shi, D.; Xiao, M.; Jiang, L.; Tian, J.; Zhang, G.; Liu, Z.; Zhang, X.; Zhang, D. Photo-/Thermal-Responsive Field-Effect Transistor upon Blending Polymeric Semiconductor with Hexaarylbiimidazole toward Photonically Programmable and Thermally Erasable Memory Device. *Adv. Mater.* **2019**, *31* (44), No. e1902576.

(12) Furukawa, H.; Cordova, K. E.; O'Keeffe, M.; Yaghi, O. M. The Chemistry and Applications of Metal-Organic Frameworks. *Science* **2013**, *341* (6149), 1230444.

(13) Karmakar, A.; Samanta, P.; Desai, A. V.; Ghosh, S. K. Guest-Responsive Metal-Organic Frameworks as Scaffolds for Separation and Sensing Applications. *Acc. Chem. Res.* **2017**, *50* (10), 2457−2469.

(14) Li, Z.; Wang, G.; Ye, Y.; Li, B.; Li, H.; Chen, B. Loading Photochromic Molecules into a Luminescent Metal-Organic Framework for Information Anticounterfeiting. *Angew. Chem., Int. Ed.* **2019**, *58* (50), 18025−18031.

(15) Sussardi, A.; Hobday, C. L.; Marshall, R. J.; Forgan, R. S.; Jones, A. C.; Moggach, S. A. Correlating Pressure-Induced Emission Modulation with Linker Rotation in a Photoluminescent MOF. *Angew. Chem., Int. Ed.* **2020**, *59* (21), 8118−8122.

(16) Jia, W.; Wu, B.; Sun, S.; Wu, P. Interfacially stable MOF nanosheet membrane with tailored nanochannels for ultrafast and thermo-responsive nanofiltration. *Nano Res.* **2020**, *13* (11), 2973−2978.

(17) Lashkari, E.; Wang, H.; Liu, L.; Li, J.; Yam, K. Innovative application of metal-organic frameworks for encapsulation and controlled release of allyl isothiocyanate. *Food Chem.* **2017**, *221*, 926−935.

(18) Li, D.; Yu, S. H.; Jiang, H. L. From UV to Near-Infrared Light-Responsive Metal-Organic Framework Composites: Plasmon and Upconversion Enhanced Photocatalysis. *Adv. Mater.* **2018**, *30* (27), No. e1707377.

(19) Haldar, R.; Heinke, L.; Wöll, C. Advanced Photoresponsive Materials Using the Metal-Organic Framework Approach. *Adv. Mater.* **2020**, *32* (20), No. e1905227.

(20) Eichler, C.; Razkova, A.; Muller, F.; Kopacka, H.; Huppertz, H.; Hofer, T. S.; Schwartz, H. A. Paving the Way to the First Functional Fulgide@MOF Hybrid Materials. *Chem. Mater.* **2021**, *33* (10), 3757−3766.

(21) Schwartz, H. A.; Ruschewitz, U. Photoactive Molecules within MOFs. In Dyes and Photoactive Molecules in Microporous Systems. Martinez, V., Arbeloa, F. L., Eds.; Vol. *183*, 2020; pp 105−153.

(22) Schwartz, H. A.; Werker, M.; Tobeck, C.; Christoffels, R.; Schaniel, D.; Olthof, S.; Meerholz, K.; Kopacka, H.; Huppertz, H.; Ruschewitz, U. Novel Photoactive Spirooxazine Based Switch@MOF Composite Materials. *ChemPhotoChem* **2020**, *4* (3), 195−206.

(23) Wu, M. X.; Yang, Y. W. Metal-organic framework (MOF)-based drug/cargo delivery and cancer therapy. *Adv. Mater.* **2017**, *29* (23), 1606134.

(24) Qin, P.; Okur, S.; Li, C.; Chandresh, A.; Mutruc, D.; Hecht, S.; Heinke, L. A photoprogrammable electronic nose with switchable selectivity for VOCs using MOF films. *Chem. Sci.* **2021**, *12* (47), 15700−15709.

(25) Wen, H.; Liu, G.; Qi, S.-C.; Gu, C.; Yang, T.; Tan, P.; Sun, L.-B. Photo-Switchable Phosphotungstic Acid Active Sites in Metal-Organic Frameworks for Tailorable Deacetalization Reaction. *J. Mater. Chem. A* **2023**, *11* (13), 6869−6876.

(26) Li, C.; Zhang, Z.; Heinke, L. Nanoporous Metal-Organic Framework Thin Films with Embedded Fulgide for Light-Modulated Guest Adsorption and Diffusion. *Langmuir* **2022**, *38* (43), 13103−13108.

(27) Chen, X.-M.; Tong, M.-L. Solvothermal in situ metal/ligand reactions: a new bridge between coordination chemistry and organic synthetic chemistry. *Acc. Chem. Res.* **2007**, *40* (2), 162−170.

(28) Shekhah, O.; Wang, H.; Kowarik, S.; Schreiber, F.; Paulus, M.; Tolan, M.; Sternemann, C.; Evers, F.; Zacher, D.; Fischer, R. A.; Woll, C. Step-by-step route for the synthesis of metal- organic frameworks. *J. Am. Chem. Soc.* **2007**, *129* (49), 15118−15119.

(29) Gu, Z.-G.; Pfriem, A.; Hamsch, S.; Breitwieser, H.; Wohlgemuth, J.; Heinke, L.; Gliemann, H.; Wöll, C. Transparent films of metal-organic frameworks for optical applications. *Micropor. Mesopor. Mater.* **2015**, *211*, 82−87.

(30) Johannsmann, D. *The Quartz Crystal Microbalance in Soft Matter Research*; Springer: 2015; p 387.

(31) Heinke, L. Diffusion and photoswitching in nanoporous thin films of metal-organic frameworks. *J. Phys. D: Appl. Phys.* **2017**, *50*, 193004.

(32) Chui, S. S.-Y.; Lo, S. M.-F.; Charmant, J. P.; Orpen, A. G.; Williams, I. D. A chemically functionalizable nanoporous material [Cu3 (TMA) 2 ($H_2O$) 3] n. *Science* **1999**, *283* (5405), 1148−1150.

(33) Müller, K.; Vankova, N.; Schottner, L.; Heine, T.; Heinke, L. Dissolving uptake-hindering surface defects in metal-organic frameworks. *Chem. Sci.* **2019**, *10* (1), 153−160.

(34) Spiegel, S.; Wagner, I.; Begum, S.; Schwotzer, M.; Wessely, I.; Bráse, S.; Tsotsalas, M. Dynamic Surface Modification of Metal-Organic Framework Nanoparticles via Alkoxyamine Functional Groups. *Langmuir* **2022**, *38* (21), 6531−6538.

(35) Hassan, Z. M.; Weidler, P. G.; Nefedov, A.; Luo, Y.; Heißler, S.; Tsotsalas, M.; Haldar, R.; Wöll, C. Spectroscopic investigation of bianthryl-based metal-organic framework thin films and their photoinduced topotactic transformation. *Adv. Mater. Interfaces* **2022**, *9* (13), 2102441.

(36) Shekhah, O.; Wang, H.; Kowarik, S.; Schreiber, F.; Paulus, M.; Tolan, M.; Sternemann, C.; Evers, F.; Zacher, D.; Fischer, R. A.; Wöll, C. Step-by-step route for the synthesis of metal-organic frameworks. *J. Am. Chem. Soc.* **2007**, *129* (49), 15118−15119.

(37) Delen, G.; Monai, M.; Meirer, F.; Weckhuysen, B. M. *In situ* Nanoscale Infrared Spectroscopy of Water Adsorption on Nanois-

lands of Surface-Anchored Metal-Organic Frameworks. *Angew. Chem.-Int. Ed.* **2021**, *60* (3), 1620−1624.
(38) Wang, Z.; Weidler, P. G.; Azucena, C.; Heinke, L.; Wöll, C. Negative, anisotropic thermal expansion in monolithic thin films of crystalline metal-organic frameworks. *Micropor. Mesopor. Mater.* **2016**, *222*, 241−246.
(39) Zybaylo, O.; Shekhah, O.; Wang, H.; Tafipolsky, M.; Schmid, R.; Johannsmann, D.; Wöll, C. A novel method to measure diffusion coefficients in porous metal-organic frameworks. *Phys. Chem. Chem. Phys.* **2010**, *12* (28), 8092−8098.
(40) Kawano, M.; Sano, T.; Abe, J.; Ohashi, Y. In situ observation of molecular swapping in a crystal by X-ray analysis. *Chem. Lett.* **2000**, *29* (12), 1372−1373.
(41) Crank, J. *The Mathematics of Diffusion*; Oxford University Press: 1979.
(42) Ruthven, D. M.; Kärger, J.; Theodorou, D. N. *Diffusion in Nanoporous Materials*; John Wiley & Sons: 2012.
(43) Wang, Z.; Grosjean, S.; Bräse, S.; Heinke, L. Photoswitchable Adsorption in Metal-Organic Frameworks Based on Polar Guest-Host Interactions. *ChemPhysChem* **2015**, *16* (18), 3779−3783.
(44) Müller, K.; Helfferich, J.; Zhao, F. L.; Verma, R.; Kanj, A. B.; Meded, V.; Bléger, D.; Wenzel, W.; Heinke, L. Switching the Proton Conduction in Nanoporous, Crystalline Materials by Light. *Adv. Mater.* **2018**, *30* (8), 1706551.
(45) Hibbe, F.; Chmelik, C.; Heinke, L.; Pramanik, S.; Li, J.; Ruthven, D. M.; Tzoulaki, D.; Kärger, J. The Nature of Surface Barriers on Nanoporous Solids Explored by Microimaging of Transient Guest Distributions. *J. Am. Chem. Soc.* **2011**, *133* (9), 2804−2807.
(46) Heinke, L.; Kärger, J. Correlating Surface Permeability with Intracrystalline Diffusivity in Nanoporous Solids. *Phys. Rev. Lett.* **2011**, *106* (7), 074501.
(47) Wang, R.; Bukowski, B. C.; Duan, J.; Sheridan, T. R.; Atilgan, A.; Zhang, K.; Snurr, R. Q.; Hupp, J. T. Investigating the Process and Mechanism of Molecular Transport within a Representative Solvent-Filled Metal-Organic Framework. *Langmuir* **2020**, *36* (36), 10853−10859.
(48) Bukowski, B. C.; Son, F. A.; Chen, Y. W.; Robison, L.; Islamoglu, T.; Snurr, R. Q.; Farha, O. K. Insights into Mass Transfer Barriers in Metal-Organic Frameworks. *Chem. Mater.* **2022**, *34* (9), 4134−4141.
(49) Heinke, L.; Gu, Z.; Wöll, C. The surface barrier phenomenon at the loading of metal-organic frameworks. *Nat. Commun.* **2014**, *5*, 4562.